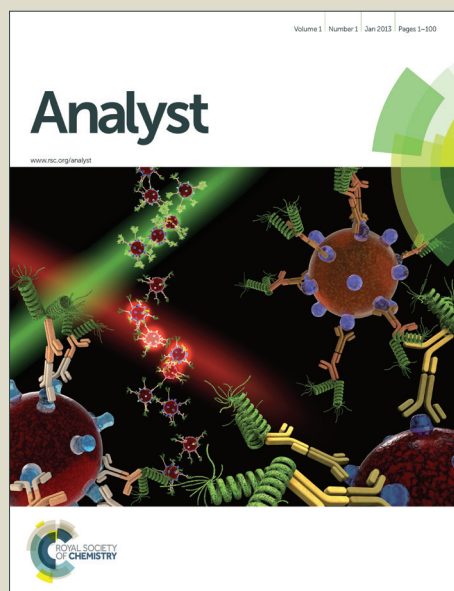# Analyst

Accepted Manuscript

This is an *Accepted Manuscript*, which has been through the Royal Society of Chemistry peer review process and has been accepted for publication.

Accepted Manuscripts are published online shortly after acceptance, before technical editing, formatting and proof reading. Using this free service, authors can make their results available to the community, in citable form, before we publish the edited article. We will replace this *Accepted Manuscript* with the edited and formatted *Advance Article* as soon as it is available.

You can find more information about *Accepted Manuscripts* in the **Information for Authors**.

Journal Name

ARTICLE

Real-time detection of hypochlorite in tap water and biological samples by a colorimetric, ratiometric and near-infrared fluorescent turn-on probe†

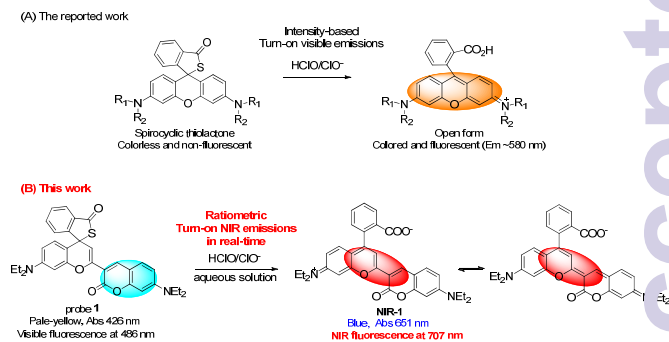Shuangshuang Ding, ‡ Qiong Zhang, ‡ Shuanghong Xue and Guoqiang Feng [*]

In this paper, we report a highly selective and sensitive ratiometric NIR fluorescent probe that can be used for real-time detection of the biologically important hypochlorite with colorimetric and significant NIR fluorescent turn-on signal changes at NIR excitation wavelength. In addition, experiments showed that this probe can be applied to detect hypochlorite in tap water, serum samples, and living cells with low cytotoxicity.

Introduction

Recently, much effort has been devoted for developing fluorescent probes for imaging hypochlorous acid (HClO)/ hypochlorite (ClO⁻) because they are biologically important reactive oxygen species (ROS) and play crucial roles in the innate immune system.[1] Regulated generation of HClO is required for the host to control the invading microbes; however, increasing evidences showed that abnormal HClO production derived from phagocytes can lead to many diseases, such as atherosclerosis, arthritis, kidney disease and cancers.[2] Due to the highly reactive and short-lived nature of HClO/ClO⁻ in living systems,[3] a practically useful fluorescent probe for bioimaging of hypochlorite in biological samples should be selective, sensitive, fast-responsive, and ideally, without any delay to show reliable signal changes.

It is well known that ratiometric fluorescent probes are more reliable over intensity-based probes because they can eliminate most or all ambiguities by self-calibration at two emission bands,[4] while near-infrared (NIR, 650-900 nm) fluorescent probes are more suitable for biological imaging applications, because they produce lower background fluorescence with less scattering, penetrate much deeper into tissues than UV and visible light and cause less damage to biological samples.[5] More practically, ratiometric fluorescent probes with NIR fluorescent turn-on property are highly desirable. In the past few years, many fluorescent probes have been developed for HClO/ClO⁻ with high selectivity;[6-8] however, most of them are intensity-based and show fluorescent signal changes only in the UV/visible region, which certainly limits their applications. Besides, ratiometric[9-10] and NIR[11] fluorescent probes for HClO/ClO⁻ are rarely reported, and as far as we know,

ratiometric probes with turn-on NIR fluorescence changes for HClO/ClO⁻ have not been reported yet. In addition, most of the reported fluorescent probes for HClO/ClO⁻ showed a delayed response time, which made them not suitable for a real-time detection of the transient HClO/ClO⁻ in living systems.

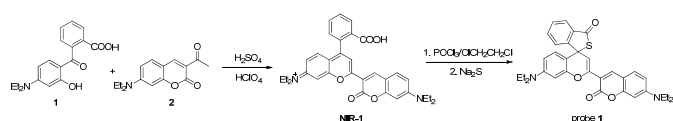Scheme 1. Thiolactone, Probe **1** and Sensing of HClO/ClO⁻.

Herein, we report a real-time ratiometric probe with NIR fluorescent turn-on changes for HClO/ClO⁻ (probe **1** in Scheme 1). This probe uses a previously reported laser dye **NIR-1**, which has the following attractive properties. First, it shows NIR absorption and emission with good fluorescence quantum yield (Φ for **NIR-1** in 20 mM PBS buffer containing 30% CH₃CN at pH 7.4 was determined to be 0.19, using rhodamine B as standard). Second, the dye contains a semi-rhodamine structure, which retained the unique merits of the widely-used rhodamine dyes, i.e. the carboxylic acid functional group can be operated as an effective fluorescence switch by the spirocyclization mechanism.[13] More importantly, **NIR 1** contains a coumarin fluorophore, which can emit fluorescence

even in its spirocyclic form. All these merits afford **NIR-1** an ideal platform to construct ratiometric NIR fluorescent probes.[14] Inspired by the previously reported thiolactones of rhodamine as good intensity-based fluorescent probes for rapid detection of HClO/ClO⁻ (Scheme 1A),[8b-d] we envisioned that probe **1**, the thiolactone of **NIR-1** should be a good ratiometric NIR fluorescent probe for HClO/ClO⁻ (Scheme 1B). Indeed, probe **1** was found to show excellent sensing properties for HClO/ClO⁻ under mild conditions, including high selectivity and sensitivity, rapid response within seconds with ratiometric and significant NIR fluorescence turn-on signal changes. In addition, probe **1** can be applied to detect ClO⁻ in tap water samples and biological samples (serum and living cells) with low cytotoxicity. Although thiolactone-based probes have also been reported to sense Hg^{2+},[14a, 15] Hg^{2+} is not a common existing in living systems. Therefore, probe **1** holds great potential as a practical tool for detection of HClO/ClO⁻ in biological samples, especially considering its rapid response and NIR fluorescent turn-on property for HClO/ClO⁻.

Results and discussion

1. Probe synthesis.

Probe **1** can be readily synthesized from the known compound **1** and **2** according to the route outlined in Scheme 2,[14a] and its structure was confirmed by ^{1}H NMR, ^{13}C NMR, MS, HR-MS and elemental analysis. The experimental details and structure characterizations are given in the experimental section and in the ESI†.

Scheme 2. Synthesis of **NIR-1** and Probe **1**.

2. The sensing property of probe 1 for HClO/ClO⁻.

The sensing ability of probe **1** was investigated in PBS buffer (20 mM, pH 7.4, containing 30% CH_3CN, v/v) at 25 °C. Initially, the response of probe **1** to various analytes including reactive oxygen/nitrogen species (ROS/RNS, such as ClO⁻, H_2O_2, NO_2^-, •OH, $^tBuOO^•$, $ROO^•$, NO, HNO, $O_2^{•-}$ and $ONOO^-$), anion species (F⁻, Cl⁻, Br⁻, I⁻, NO_3^-, AcO⁻, SCN⁻, CO_3^{2-}, SO_4^{2-}, SO_3^{2-}, $S_2O_3^{2-}$, CN⁻, HS⁻ and PO_4^{3-}), biothiols (glutathione (GSH), homocysteine (Hcy), cysteine (Cys)), two representative amino acids (phenylalanine (Phe) and glycine (Gly)), and other nucleophilic agents ($H_2NCH_2CH_2NH_2$, $HOCH_2CH_2NH_2$, $C_6H_5NH_2$ and $C_6H_5CH_2NH_2$) was tested to see whether it can detect ClO⁻ selectively. A colorimetric assay showed that only addition of ClO⁻ (NaClO was used) induced an immediate and highly apparent color change to the probe **1** solution (from pale-yellow to blue), while all the other analytes showed no effect (Fig. S1a, ESI†). A selective emission color change of the probe **1** solution was also observed only to ClO⁻ (Fig. S1b, ESI†). This indicates that probe **1** can be used as a

dual selective colorimetric and fluorescent sensor to detect ClO⁻. The spectra changes of probe **1** toward these analytes further proved the selectivity. As shown in Fig. 1, in the absorption spectra, only upon addition of ClO⁻, the probe **1** solution showed a large red shift of the absorption peak from 427 nm to 651 nm, which is in good agreement with the observed color change (inserted in Fig. 1a). In the fluorescence spectra, as expected, the probe **1** solution shows the typical blue-green fluorescence of the coumarin moiety (λ_{em} 486 nm with λ_{ex} 430 nm, Φ = 0.080, using rhodamine B as standard) and almost zero background fluorescence above 650 nm. Upon addition of ClO⁻, the fluorescence at 486 nm was significantly quenched, accompanied by a strong NIR fluorescence enhancement at 707 nm with λ_{ex} at 650 nm. In contrast, other analytes caused negligible changes to the probe **1** solution (Fig. 1b). Moreover, detection of ClO⁻ using probe **1** in the presence of other analytes including other ROS/RNS is still effective (Fig. S2, ESI†). All these experiments clearly indicate that probe **1** is highly selective for ClO⁻.
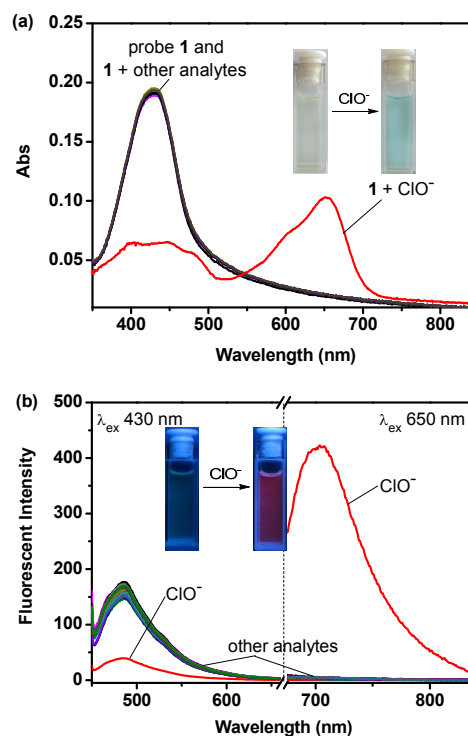

Fig. 1 (a) Absorption and (b) fluorescent spectral changes of probe **1** (5 μM) upon addition of ClO⁻ (30 μM) and various other analytes (100 μM of each, except 1 mM of GSH). Other analytes include: none, $ONOO^-$, $^tBuOO^•$, •OH, NO, HNO, H_2O_2, $ROO^•$, $O_2^{•-}$, NO_2^-, F⁻, Cl⁻, Br⁻, I⁻, NO_3^-, AcO⁻, SCN⁻, CO_3^{2-}, SO_4^{2-}, SO_3^{2-}, $S_2O_3^{2-}$, CN⁻, HS⁻, PO_4^{3-}, $H_2NCH_2CH_2NH_2$, $HOCH_2CH_2NH_2$, $C_6H_5NH_2$, $C_6H_5CH_2NH_2$, GSH, Hcy, Cys, Phe, Gly. All experiment was performed in PBS buffer (20 mM, pH 7.4) with 30% CH_3CN at 25 °C and each spectrum was obtained 1 min after addition of each analyte. Fluorescent spectral were recorded with λ_{ex} = 430 nm and 650 nm, respectively.

It is noteworthy that the color and optical spectral changes of probe **1** toward ClO⁻ occur immediately (Fig. S3, ESI†). This rapid response indicates that probe **1** is very sensitive to ClO⁻,

which is highly favourable for a real-time detection. To obtain further insight into the sensitivity of probe **1** for ClO⁻, the fluorescence spectra of probe **1** upon titration with different concentrations of NaClO were recorded. As shown in Fig. 2a, upon progressive addition of ClO⁻, the fluorescence of the probe **1** solution at 486 nm (λ_{ex} 430 nm) gradually decreased with the simultaneous enhancement of the NIR emission at 707 nm (λ_{ex} 650 nm) until they reached a plateau after the addition of more than five equiv of ClO⁻ (Fig. S4, ESI†). It should be noted that under these experimental conditions, after addition of ClO⁻ (30 μM), the emission intensities of the probe **1** (5 μM) solution at 707 and 486 nm changed from 3.7523 and 170.5610 to 416.5987 and 38.9819, respectively. As a result, the ratio of emission intensities at I_{707}/I_{486} varied from 0.0220 to 10.6871, corresponding to a 486-fold enhancement, which is remarkable. In addition, excellent linear calibration graphs of the NIR fluorescence (I_{707}) and the ratiometric responses (I_{707}/I_{486}) to the ClO⁻ concentrations from 0 to 15 μM can be observed (Fig. 2b and Fig. S5, ESI†). The detection limit of probe **1** for ClO⁻ was measured to be about 40 nM based on signal-to-noise ratio (S/N) = 3 under the test conditions. Clearly, this result indicates that probe **1** can be employed to detect ClO⁻ quantitatively with excellent sensitivity. Thus, a highly selective and sensitive colorimetric and ratiometric probe for rapid detection of ClO⁻ with significant NIR fluorescence turn-on responses was established.
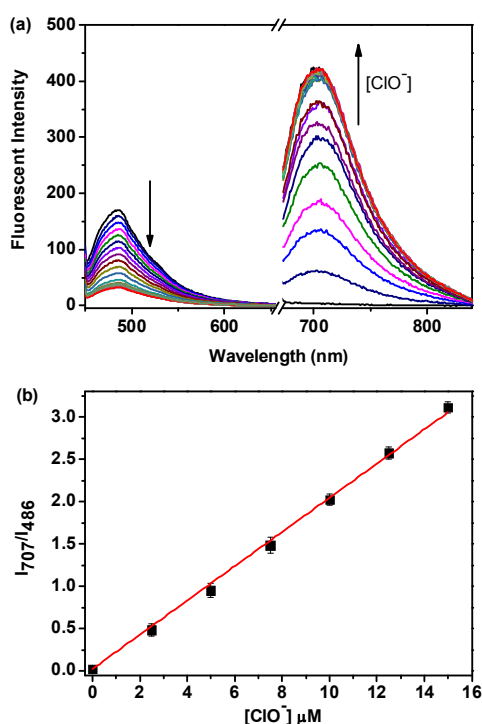

Fig. 2 (a) Fluorescent spectral changes of probe **1** (5 μM) in PBS buffer (20 mM, pH 7.4, with 30% CH₃CN, v/v) at 25 °C upon addition of ClO⁻ (0-50 μM). Excitation wavelength was used at 430 nm and 650 nm for the visible and NIR part, respectively. (b) Linear relationship of the ratiometric responses (I_{707}/I_{486}) as a function of ClO⁻ concentration from 0 to 15 μM. The data were reported as the mean ± standard

deviation of triplicate experiments and can be fitted by equation y = 0.023 + 0.203×[NaClO] with R^2 = 0.9992.

3. The effect of pH and the sensing mechanism.

The effect of pH for probe **1** towards ClO⁻ detection was investigated. As shown in Fig. S6 (ESI†), we can see that without ClO⁻, both the absorbance and the fluorescence of probe **1** showed very small changes to the pH variations in a wide range (from 2 to 10). However, in the presence of ClO⁻, the absorbance and the fluorescence intensity of probe **1** showed distinct changes over a wide pH range (from 3 to 9), which indicates that probe **1** can be used to detect ClO⁻ over a wide pH range. Notably, the NIR fluorescence change of probe **1** to NaClO is most sensitive at pH about 5. Indeed, the saturation occurs at addition of only about three equiv. of NaClO to probe **1** and the detection limit was reduced to be 21 nM at pH = 5.0 (Fig. S7, ESI†). Considering HClO is more preferably generated by the catalysis of myeloperoxidase (MPO) under acidic conditions (pH ~5.0) in biological systems,[16] probe **1** has great potential for HClO detection in living systems.

According to the previously reported thiolactone-based fluorescent probes for ClO⁻,[8b-d] the optical changes of probe **1** to ClO⁻ suggest that the spirocyclic thiolactone of probe **1** was oxidized by ClO⁻ to form the ring-opened NIR fluorescent **NIR-1**. To confirm this, the fluorescent reaction product of probe **1** with NaClO was isolated and subjected to analysis, and indeed, TLC, ¹H NMR, and MS analysis clearly showed that **NIR-1** was formed (Fig. S8-10, ESI†). Thus, the sensing mechanism of probe **1** for ClO⁻ is most likely the process as shown in Scheme 1(B). However, due to the unique structure of probe **1**, it should be noted that probe **1** showed significantly different sensing properties, i.e., a ratiometric and NIR fluorescent turn-on sensing process for ClO⁻, while those previously reported thiolactone-based fluorescent probes[8b-d] for ClO⁻ only showed a visible fluorescent turn-on sensing process. Obviously, probe **1** is more attractive. In addition, as indicated in Table S1 (ESI†), probe **1** showed excellent sensing performance compared to many other recently developed fluorescent probes for ClO⁻, which indicates that it is promising for practical analysis.

4. The potential applications of probe 1.

Prompted by its high sensitivity and selectivity, the practical application of probe **1** was then investigated. It is well known that a small amount of residual hypochlorite may exist in tap water after chlorine disinfection. Since probe **1** in the deionized water shows almost no background fluorescence in the NIR region, we applied probe **1** to determine the concentration of ClO⁻ in the tap water of our lab. As shown in Fig. S11 (ESI†), when the deionized water was replaced by the tap water (pH was adjusted to 7.4), significant NIR fluorescence enhancement can be observed. In contrast, probe **1** shows almost no response to the boiled tap water. This result indicates that probe **1** can be used to detect ClO⁻ in real tap water samples. Using the linear calibration graph in Fig. S5 (ESI†), the NIR fluorescence enhancement at 707 nm by tap water suggests that the

concentration of ClO$^-$ in the tap water sample is about 1.14 μM, which was found in good agreement with the result by a conventional titration method (Table 1). In addition, when the tap water were further spiked with NaClO at known levels (0.50 and 2.50 μM, respectively), the total concentration of ClO$^-$ in each sample was measured by the fluorescence responses of probe **1** at 707 nm, and the results showed that the recoveries of ClO$^-$ are rather satisfactory (Table 1). Therefore, probe **1** has great potential for quantitative detection of ClO$^-$ in real water samples. In addition, we also successfully applied the convenient test strips containing probe **1** to detect ClO$^-$ in water samples by the naked eye, and the discernible level of ClO$^-$ could be as low as 50 μM (Fig. S12, ESI†).

Table 1. Determination of ClO$^-$ concentration in tap water sample of the lab

sample	titration method^a (μM)	this method (μM)	added (μM)	found (μM)	recovery (%)
Tap water in our lab	1.1 ± 0.1	1.14 ± 0.04	0.50	1.67 ± 0.05	101.8 ± 1.2
			2.50	3.62 ± 0.06	99.5 ± 1.2

^{a}Note: The titration method is based on the following two equations: (1) $2H^+ + ClO^- + 2I^- = I_2 + Cl^- + H_2O$; (2) $I_2 + 2S_2O_3^{2-} = S_4O_6^{2-} + 2I^-$, and use starch as indicator (Ref: Standard examination methods for drinking water-Disinfection by products parameters GB/T 5750.10-2006(1), General Administration of Quality Supervision, Inspection and Quarantine of the People's Republic of China, 2006.). The results shown in the Table 1 were reported as the mean ± standard deviation of triplicate experiments.

We also investigated the utility of probe **1** for determination of HClO in biological samples. Detection of HClO in commercially available fetal bovine serum (FBS) by probe **1** was first evaluated. In this investigation, the received FBS sample was directly diluted ten times with CH$_3$CN-PBS buffer. As shown in Fig. S13 (ESI†), incubation of this diluted FBS sample with probe **1** (5 μM) showed no fluorescence changes in the NIR region even the incubation time was prolonged to more than 10 min (Fig. S13a, ESI†). However, addition of NaClO (30 μM) to this solution resulted in significant NIR fluorescence enhancement immediately (Fig. S13b, ESI†). In addition, when this FBS solution containing NaClO with different concentrations (0, 3, 6, 9, 12, and 15 μM) was incubated with 5 μM probe **1**, the NIR fluorescence intensity at 707 nm was found to enhance linearly with the increased concentration of HClO (Fig. S13c and 13d, ESI†), and the detection limit for NaClO in this serum sample was calculated to be about 68 nM (S/N=3). These results clearly indicate that probe **1** is able to detect HClO in serum samples sensitively and quantitatively.

Fluorescent imaging of ClO$^-$ in living cells was also investigated. As shown in Fig. 3, when HeLa cells were incubated with probe **1** (20 μM), strong green fluorescence was observed (B) and no fluorescence can be observed in the red channel (C), which agrees well with the fluorescence of probe **1** itself, indicating that probe **1** is cell-permeable. However, when HeLa cells were pre-incubated with probe **1** and then incubated

with NaClO (100 μM) for 15 min, an obvious fluorescence decrease in the green channel (B1) and a significant fluorescence increase in the red channel (C1) were observed. This is a clear ratiometric detection process, and is in good agreement with the ClO$^-$-induced ratiometric fluorescence response aforementioned. In addition, the cytotoxicity of probe **1** in HeLa cells was investigated by MTT assays, and the results showed that probe **1** is of low cytotoxicity to cultured cells (Fig. S14, ESI†). These data clearly indicate that probe **1** can be applied to detect exogenous hypochlorite ratiometrically in living cells.
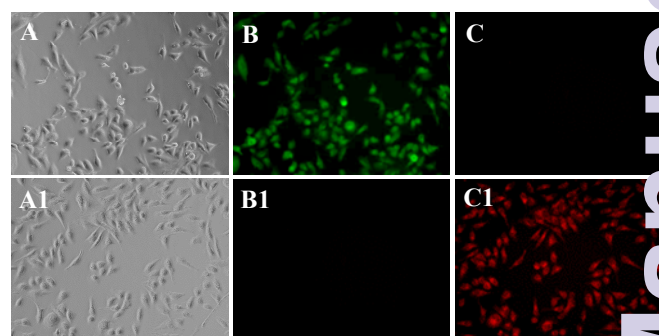

Fig. 3 Imaging of ClO$^-$ in HeLa Cells by probe **1**. Top (A, B, and C): HeLa cells were incubated with probe **1** (20 μM) for 45 min. Bottom (A1, B1, and C1): HeLa cells were incubated with probe **1** (20 μM) for 45 min prior to incubate with NaClO (100 μM) for 15 min. A and A1: Bright field imaging; B and B1: Fluorescence imaging from the green channel (excitation wavelength was set at 450-490 nm); C and C1: Fluorescence imaging from the red channel (excitation wavelength was set at 515-560 nm).
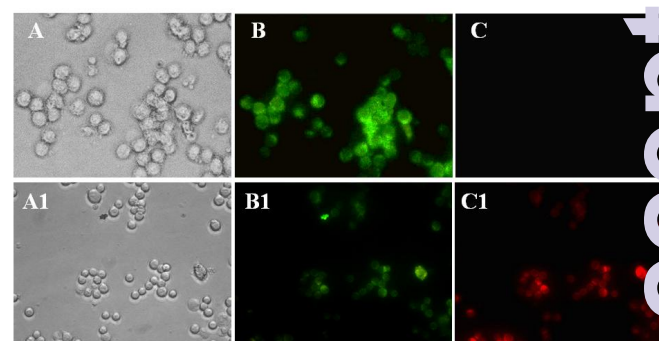

Fig. 4 Imaging of endogenous ClO$^-$ in Raw264.7 Cells by probe **1**. Top (A, B, and C): Raw264.7 cells were incubated with probe **1** (20 μM) for 40 min. Bottom (A1, B1, and C1): Raw264.7 cells were incubated with LPS (1 μg/mL) for 24 h and then further incubated with PMA (1 μg/mL) for 2 h and probe **1** (20 μM) for 30 min. A and A1: Bright field imaging; B and B1: Fluorescence imaging from the green channel (excitation wavelength was set at 450-490 nm); C and C1: Fluorescence imaging from the red channel (excitation wavelength was set at 515-560 nm).

Detection of endogenous HClO in living cells by probe **1** was also investigated. It was reported that RAW264.7 macrophage cells can produce endogenous HOCl when stimulated by lipopolysaccharide (LPS) and phorbol myristate acetate (PMA).[6j-k,10c,11c] RAW264.7 cells were therefore used for this study. As shown in Fig. 4, when the living RAW264.7 cells were loaded with probe **1**, only green fluorescence can be observed (Fig. 4B). However, after the cells have been

incubated with LPS (1 μg/mL) for 24 h, and then further incubated with PMA (1 μg/mL) for 2 h and probe **1** (20 μM) for 30 min, an fluorescence decrease in the green channel (B1) and a significant fluorescence increase in the red channel (C1) were observed. These data indicate that probe **1** is able to fluorescence image endogenously produced HClO in the living RAW264.7 cells.

Experimentals

General

Unless otherwise stated, all chemicals were purchased from commercial suppliers and used without further purification. All solvents were purified prior to use. Distilled water was used after passing through a water ultrapurification system. TLC analysis was performed using precoated silica plates. ^1H NMR and ^{13}C NMR spectra were recorded on a Varian Mercury 600 or 400 spectrometer, and resonances (δ) are given in parts per million relative to tetramethylsilane (TMS). Coupling constants (J values) are reported in hertz. IR spectra were recorded on a FT-IR spectrophotometer as KBr pellets and were reported in cm^{-1}. The low-resolution MS spectra were performed on an electron ionization mass spectrometer. HR-MS data were obtained with an LC/Q-TOF MS spectrometer. UV-vis and fluorescence spectra were recorded at 25°C on a UV-vis spectrophotometer and a fluorescence spectrophotometer with a temperature controller, respectively. Standard quartz cuvettes with a 10 mm lightpath were used for all optical spectra measurements. Cell imaging was performed in an inverted fluorescence microscopy with a 20× and a 40×objective lens for HeLa cells and Raw264.7 cells, respectively.

Synthesis of NIR-1. Compound **1**[17] (330 mg, 1 mmol) and **2**[18] (297 mg, 1 mmol) were dissolved in conc. H_2SO_4 (5 mL), then the solution was stirred at 90 °C for 6 h. After cooling to room temperature, the reaction mixture was poured into ice (10 g) and followed by addition of perchloric acid (70%, 0.5 mL). The resulting green residue was collected by filtration, washed with cold water to yield the crude NIR-1, which was further purified by recrystallization from ethanol to afford the pure product (237 mg, yield 42%) as a blue solid. Mp: 212-218 °C. TLC (silica plate): R_f 0.17 (petroleum ether: ethyl acetate 2:1, v/v). ^1H NMR (400 MHz, d_6-DMSO): δ 9.15 (d, J = 6.7 Hz, 1H), 8.16 (d, J = 7.7 Hz, 1H), 8.09 (s, 1H), 7.85 (t, J = 7.5 Hz, 1H), 7.77 (dd, J = 17.3, 8.7 Hz, 2H), 7.52 (d, J = 7.6 Hz, 1H), 7.29 (d, J = 9.5 Hz, 2H), 7.21 (d, J = 8.7 Hz, 1H), 7.00 (d, J = 9.1 Hz, 1H), 6.74 (s, 1H), 3.67 (d, J = 6.2 Hz, 4H), 3.59 (d, J = 6.2 Hz, 4H), 1.25 (s, 6H), 1.18 (t, J = 6.8 Hz, 6H). ^{13}C NMR (100 MHz, DMSO-d_6): δ 166.9, 166.8, 161.4, 158.1, 155.2, 154.7, 145.9, 135.9, 133.1, 132.8, 130.9, 130.8, 130.6, 130.5, 129.7, 129.4, 117.4, 115.7, 112.0, 111.6, 109.7, 109.4, 105.2, 96.5, 96.2, 54.9, 45.6, 45.2, 12.6. IR (KBr, cm^{-1}) 3445 (br), 3081, 2981, 1721, 1624, 1568, 1538, 1509, 1483, 1432, 1404, 1388, 1329, 1274, 1252, 1214, 1200, 1171, 1130, 1070, 768, 718. EI-MS: m/z found 538.54 (M^+-HClO$_4$). HR-MS: calcd for $C_{33}H_{33}N_2O_5^+$ (M -HClO$_4$+H$^+$)$^+$, 537.23840; found 537.23754.

Synthesis of Probe 1.[14a] Compound **NIR-1** (318 mg, 0.5 mmol) was dissolved in dry 1,2-dichloromethane (4 mL), stirred at room temperature, then POCl$_3$ (0.2 mL) was slowly added over a period of 5 min, and the mixed solution was heated to reflux for 4 h. After cooling, the reaction mixture was concentrated under vacuum to obtain crude acid chloride of **NIR-1**, which was directly used for next step.

The crude acid chloride was dissolved in 5 mL of saturated Na$_2$S aqueous solution, and then the solution was stirred for 3 h at room temperature. The mixture was extracted with ethyl acetate (10 mL × 3), and the combined organic phase was dried over Na$_2$SO$_4$ and the crude product was concentrated under vacuum, then purified by flash chromatography with CH$_2$Cl$_2$ as the eluent to afford probe **1** as a yellow solid (82 mg, yield 30%). Mp: 214-216 °C. TLC (silica plate): R_f 0.78 (petroleum ether: ethyl acetate 2:1, v/v). ^1H NMR (400 MHz, CDCl$_3$): δ 8.26 (s, 1H), 7.82 (d, J = 7.7 Hz, 1H), 7.57 (t, J = 7.4 Hz, 1H), 7.47 − 7.37 (m, 3H), 6.69 (d, J = 11.2 Hz, 3H), 6.49 (s, 1H), 6.36 (s, 2H), 3.43 (dd, J = 14.1, 7.0 Hz, 4H), 3.35 (d, J = 7.0 Hz, 4H), 1.20 (dt, J = 17.1, 6.9 Hz, 12H). ^{13}C NMR (100 MHz, DMSO-d_6): δ 196.9, 159.0, 157.0, 155.8, 151.8, 150.9, 148.7, 144.2, 139.0, 134.8, 133.8, 129.5, 129.3, 128.1, 127.1, 122.5, 111.6, 109.0, 108.8, 108.0, 107.1, 104.1, 97.2, 96.4, 60.8, 44.6, 44.1, 12.4, 12.2. IR (KBr, cm^{-1}) 2975, 2926, 1719, 1686, 1624, 1590, 1516, 1469, 1454, 1418, 1376, 1355, 1319, 1304, 1268, 1135, 922, 795, 772. EI-MS: m/z found 552.50 (M^+). HR-MS: calcd for $C_{33}H_{33}N_2O_4S^+$ (M + H$^+$), 553.21555; found 553.21552. Elemental analysis calcd (%) for $C_{33}H_{32}N_2O_4S$ (MW. 552.5) C 71.71, H 5.84, N 5.07, S 5.80; found C 71.89, H 5.78, N 5.19, S 5.79.

Optical studies of probe 1 upon addition of various analytes. Stock solution of probe **1** and various anaylytes were prepared in HPLC grade CH$_3$CN and water, respectively, and were used freshly. ROS/RNS such as ClO$^-$, H$_2$O$_2$, NO$_2^-$, $^•$OH, ^{t}BuOO$^•$, NO, O$_2^{•-}$, and ONOO$^-$ *etc.* were prepared according to our published procedure[19a] and were used freshly. For a typical optical measurements, probe **1** was diluted to 5 μM in a PBS buffer solution (20 mM, pH 7.4, containing 30% CH$_3$CN, v/v), and 3.0 mL of the resulting solution was placed in a quartz cell and kept at 25 °C. The UV–vis or fluorescent spectra were then recorded upon addition of analytes.

Cell Culture and Bioimaging. Cells were cultured according to our published procedure.[19] For living cells imaging experiment of probe **1**, cells were incubated with 20 μM of probe **1** at 37 °C and washed three times with prewarmed PBS, and then imaged in the bright field, green channel, and red channel, respectively. For imaging of exogenous HClO, HeLa cells were pretreated with probe **1** (20 μM) for 45 min at 37 °C, washed three times with prewarmed PBS, and then incubated with NaClO (100 μM) for 15 min at 37 °C. Cell imaging was then carried out after washing cells with prewarmed PBS buffer. For imaging of endogenous HClO, the living RAW264.7 cells were treated with LPS (1 μg/mL) for 24 h and then further coincubated with PMA (1 μg/mL) for 2 h, probe **1** (20 μM) for 30 min at 37 °C. Prior to imaging, the cells

were washed three times with PBS, and the fluorescence images were acquired in an inverted fluorescence microscopy.

Conclusions

In summary, we developed a colorimetric and ratiometric NIR fluorescent probe for real-time detection of HClO/ClO⁻. The merits of this probe for HClO/ClO⁻ include high selectivity and sensitivity, rapid response within seconds with ratiometric and significant NIR fluorescence turn-on signal changes (at NIR excitation wavelength) under mild conditions over a wide pH range (4-8). In addition, this probe can be applied to detect HClO/ClO⁻ in real water samples and biological samples (serum and living cells) with low cytotoxicity. We believe that the excellent sensing properties of this probe combined with its capability of bioimaging will make it a real useful tool for further studying biological roles of hypochlorite.

Acknowledgements

Notes and references

Key laboratory of Pesticide and Chemical Biology of Ministry of Education, College of Chemistry, Central China Normal University, 152 Luoyu Road, Wuhan 430079, P. R. China. E-mail: gf256@mail.ccnu.edu.cn

‡ These authors contributed equally to this work.

† Electronic Supplementary Information (ESI) available: [Structure characterizations for **NIR-1** and probe **1**, additional optical data, and data for investigation of the sensing mechanism]. See DOI: 10.1039/b000000x/

1 (a) X. Chen, X. Tian, I. Shin and J. Yoon, *Chem. Soc. Rev.*, 2011, **40**, 4783–4804; (b) Y. M. Yang, Q. Zhao, W. Feng and F. Y. Li, *Chem. Rev.*, 2012, **113**, 192–270.

2 (a) D. I. Pattison, M. J. Davies, *Chem. Res. Toxicol.*, 2001, **14**, 1453–1464; (b) C. C. Winterbourn, A. J. Kettle, *J. Free Radical Biol. Med.*, 2000, **29**, 403–409.

3 (a) S. J. Klebanoff, *J. Leukocyte Biol.*, 2005, **77**, 598–625; (b) J. M. Albrich, C. A. McCarthy, J. K. Hurst, *Proc. Natl. Acad. Sci. USA*, 1981, **78**, 210–214.

4 M. H. Lee, J. S. Kim and J. L. Sessler, *Chem. Soc. Rev.*, 2015, **DOI:** 10.1039/C4CS00280F.

5 (a) Z. Guo, S. Park, J. Yoon and I. Shin, *Chem. Soc. Rev.*, 2014, **43**, 16–29; (b) L. Yuan, W. Lin, K. Zheng, L. He and W. Huang, *Chem. Soc. Rev.*, 2013, **42**, 622–661.

6 Some recent examples, see (a) J. J. Hu, N.-K. Wong, Q. Gu, X. Bai, S. Ye and D. Yang, *Org. Lett.*, 2014, **16**, 3544–3547; (b) S.-R. Liu and S.-P. Wu, *Org. Lett.*, 2013, **15**, 878–881; (c) B. Wang, P. Li, F. Yu, P. Song, X. Sun, S. Yang, Z. Lou and K. Han, *Chem. Commun.*, 2013, **49**, 1014–1016; (d) G. Li, D. Zhu, Q. Liu, L. Xue and H. Jiang, *Org. Lett.*, 2013, **15**, 2002–2005; (e) T. Guo, L. Cui, J. Shen, R. Wang, W. Zhu, Y. Xu and X. Qian, *Chem. Commun.*, 2013, **49**, 1862–1864; (f) M. Emrullahoğlu, M. Üçüncü and E. Karakuş, *Chem.*

Commun., 2013, **49**, 7836−7838; (g) G. Cheng, J. Fan, W. Sun, K. Sui, X. Jin, J. Wang and X. Peng, *Analyst*, 2013, **138**, 6091−6096; (h) Z. Lou, P. Li, Q. Pan and K. Han, *Chem. Commun.*, 2013, **49**, 2445–2447; (i) S. T. Manjare, J. Kim, Y. Lee and D. G. Churchill, *Org. Lett.*, 2014, **16**, 520–523; (j) S. I. Reja, V. Bhalla, A. Sharma, G. Kaur and M. Kumar, *Chem. Commun.*, 2014, **50**, 11911–11914; (k) H. Zhu, J. Fan, J. Wang, H. Mu and X. Peng, *J. Am. Chem. Soc.*, 2014, **136**, 12820–12823.

7 (a) S. Kenmoku, Y. Urano, H. Kojima and T. Nagano, *J. Am. Chem. Soc.*, 2007, **129**, 7313−7318; (b) Y. K. Yang, H. J. Cho, J. Lee, I. Shin and J. Tae, *Org. Lett.*, 2009, **11**, 859–861; (c) Q. A. Best, N. Sattenapally, D. J. Dyer, C. N. Scott and M. E. McCarroll, *J. Am. Chem. Soc.*, 2013, **135**, 13365−13370; (d) X. Wu, Z. Li, L. Yang, J. Han and S. Han, *Chem. Sci.*, 2013, **4**, 460−467.

8 (a) X. Q. Chen, X. C. Wang, S. J. Wang, W. Shi, K. Wang and H. M. Ma, *Chem.–Eur. J.*, 2008, **14**, 4719–4724; (b) X. Q. Zhan, J. H. Yan, J. H. Su, Y. C. Wang, J. He, S. Y. Wang, H. Zheng and J. G. Xu, *Sens. Actuators, B*, 2010, **150**, 774–780; (c) X. Q. Chen, K. A. Lee, E. M. Ha, K. M. Lee, Y. Y. Seo, H. K. Choi, H. N. Kim, M. J. Kim, C. S. Cho, S. Y. Lee, W. J. Lee and J. Yoon, *Chem. Commun.*, 2011, **47**, 4373–4375; (d) Q. Xu, K.-A. Lee, S. Lee, K. M. Lee, W.-J. Lee and J. Yoon, *J. Am. Chem. Soc.*, 2013, **135**, 9944−9949; (e) J.-T. Hou, M.-Y. Wu, K. Li, J. Yang, K.-K. Yu, Y.-M. Xie and X.-Q. Yu, *Chem. Commun.*, 2014, **50**, 8640–8643.

9 (a) J. Park, H. Kim, Y. Choi and Y. Kim, *Analyst*, 2013, **138**, 3368–3371; (b) Z. Lou, P. Li, P. Song and K. Han, *Analyst*, 2013, **138**, 6291–6295; (c) J. Zha, B. Fu, C. Qin, L. Zeng and X. Hu, *RSC Adv.*, 2014, **4**, 43130–43113; (d) S. Goswami, A. Manna, S. Paul, C. K. Quah and H.-K. Fun, *Chem. Commun.*, 2013, **49**, 11656–11658; (e) L. Yuan, W. Lin, J. Song and Y. Yang, *Chem. Commun.*, 2011, **47**, 12691–12693.

10 (a) L. Yuan, W. Lin, Y. Xie, B. Chen, J. Song, *Chem.–Eur. J.*, 2012, **18**, 2700−2706; (b) G. Chen, F. Song, J. Wang, Z. Yang, S. Sun, J. Fan, X. Qiang, X. Wang, B. Dou, X. Peng, *Chem. Commun.*, 2012, **48**, 2949−2951; (c) Y.-R. Zhang, X.-P. Chen, J.-S., J.-Y. Zhang, L. Yuan, J.-Y. Miao, B.-X. Zhao, *Chem. Commun.*, 2014, **50**, 14241–14244; (d) J.-T. Hou, K. Li, J. Yang, K.-K. Yu, Y.-X. Liao, Y.-Z. Ran, Y.-H. Liu, X.-D. Zhou and X.-Q. Yu, *Chem. Commun.*, 2015, **51**, 6781–6784.

11 (a) J. Shepherd, S. A. Hilderbrand, P. Waterman, J. W. Heinecke, R. Weissleder and P. Libby, *Chem. Biol.*, 2007, **14**, 1221–1231; (b) Y. Koide, Y. Urano, K. Hanaoka, T. Terai and T. Nagano, *J. Am. Chem. Soc.*, 2011, **133**, 5680−5682; (c) L. Yuan, W. Lin, Y. Yang and H. Chen, *J. Am. Chem. Soc.*, 2012, **134**, 1200−1211; (d) G. Cheng, J. Fan, W. Sun, J. Cao, C. Hu and X. Peng, *Chem. Commun.*, 2014, **50**, 1018–1020.

12 P. Czerney, G. Graneß, E. Birckner, F. Vollmer and W. Rettig, *J. Photochem. Photobiol. A*, 1995, **89**, 31–36.

13 (a) X. Chen, T. Pradhan, F. Wang, J. S. Kim and J. Yoon, *Chem. Rev.*, 2012, **112**, 1910−1956. (b) H. N. Kim, M. H. Lee, H. J. Kim, J. S. Kim and J. Yoon. *Chem. Soc. Rev.*, 2008, **37**, 1465−1472. (c) M. Beija, C. A. M. Afonso and J. M. G. Martinho, *Chem. Soc. Rev.*, 2009, **38**, 2410–2433.

14 (a) J. Liu, Y. Q. Sun, P. Wang, J. Zhang, W. Guo, *Analyst*, 2013, **138**, 2654−2660; (b) H. Lv, X.-F. Yang, Y. Zhong, Y. Guo, Z. Li and H. Li, *Anal. Chem.*, 2014, **86**, 1800–1807; (c) Y.-W. Duan, X.-F. Yang

ARTICLE

Y. Zhong, Y. Guo, Z. Li and H. Li, *Anal. Chim. Acta*, 2015, **859**, 59–65.

15 (a) W. Shi and H. Ma, *Chem. Commun.*, 2008, 1856–1858; (b) X.-Q. Zhan, Z.-H. Qian, H. Zheng, B.-Y. Su, Z. Lan and J.-G. Xu, *Chem. Commun.*, 2008, 1859–1861; (c) X. Chen, S.-W. Nam, M. J. Jou, Y. Kim, S.-J. Kim, S. Park and J. Yoon, *Org. Lett.*, 2008, **10**, 5235–5238.

16 (a) S. J. Weiss, R. Klein, A. Slivka, M. Wei, *J. Clin. Invest.*, 1982, **70**, 598−607; (*b*) P. C. Andrews and N. I. Krinsky, *J. Biol. Chem.*, 1982, **257**, 13240−13245.

17 Q.-H. Liu, J. Liu, J.-C. Guo, X.-L. Yan, D.-H. Wang, L. Chen, F.-Y. Yan and L.-G. Chen, *J. Mater. Chem.*, 2009, **19**, 2018–2025.

18 J. Wu, R. Sheng, W. Liu, P. Wang, H. Zhang and J. Ma, *Tetrahedron*, 2012, **68**, 5458–5463.

19 (*a*) D. Yu, F. Huang, S. Ding and G. Feng, *Anal. Chem.*, 2014, **86**, 8835−8841; (*b*) Y. Liu, D. Yu, S. Ding, Q. Xiao, J. Guo and G. Feng, *ACS Appl. Mater. Interfaces* 2014, **6**, 17543–17550; (*c*) D. Yu, Q. Zhang, S. Ding and G. Feng, *RSC Adv.*, 2014, **4**, 46561–46567; (*d*) Q. Zhang, D. Yu, S. Ding and G. Feng, *Chem. Commun.*, 2014, **50**, 14002–14005; (*e*) Z. Huang, S. Ding, D. Yu, F. Huang and G. Feng, *Chem. Commun.*, 2014, **50**, 9185–9187; (f) S. Xue, S. Ding, Q. Zhai, H. Zhang and G. Feng, *Biosens. Bioelectron.*, 2015, **68**, 316–321; (g) Q. Zhang, Y. Zhang, S. Ding, H. Zhang and G. Feng, *Sens. Actuators, B* 2015, **211**, 377–384.